Supporting Information

Proximity-Induced Spin Filtering in vdW CrSBr Spin-Valves with $ZrTe_5$ Barriers

Puja Kumari[1], **Anusree C.V,** and **V Kanchana**[1*]

Department of Physics, Indian Institute of Technology Hyderabad, Kandi, Medak 502 284, Telangana, India; ∗ E-mail: kanchana@phy.iith.ac.in

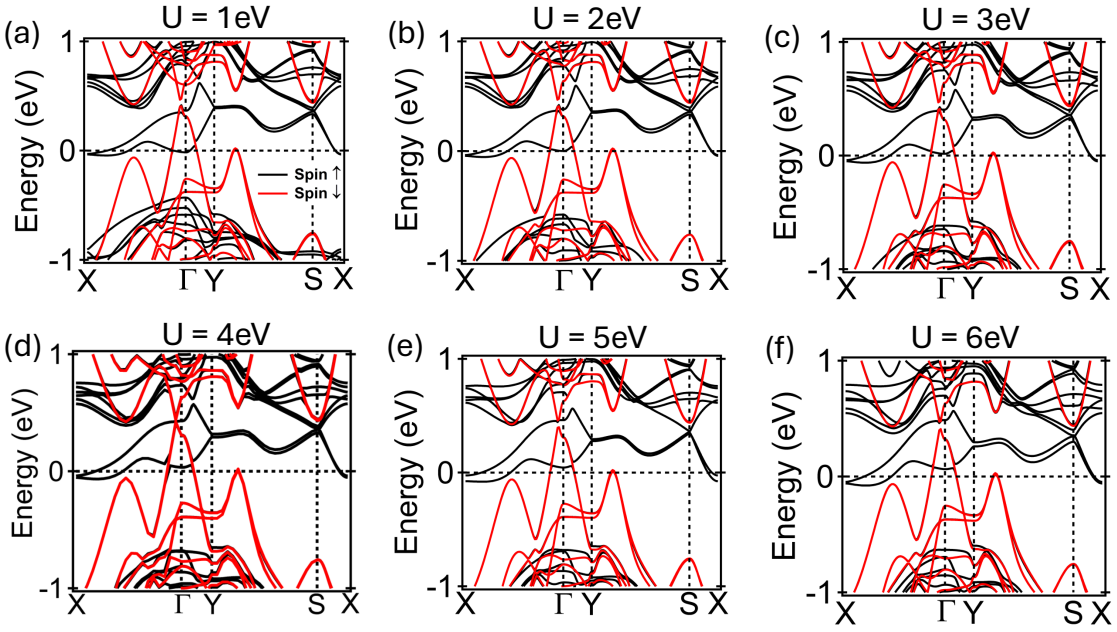

Fig. S1 Spin - polarized band structures of the $ZrTe_5$/CrSBr heterostructure calculated with varying Hubbard U values (1 eV to 6 eV) applied to Cr atoms.

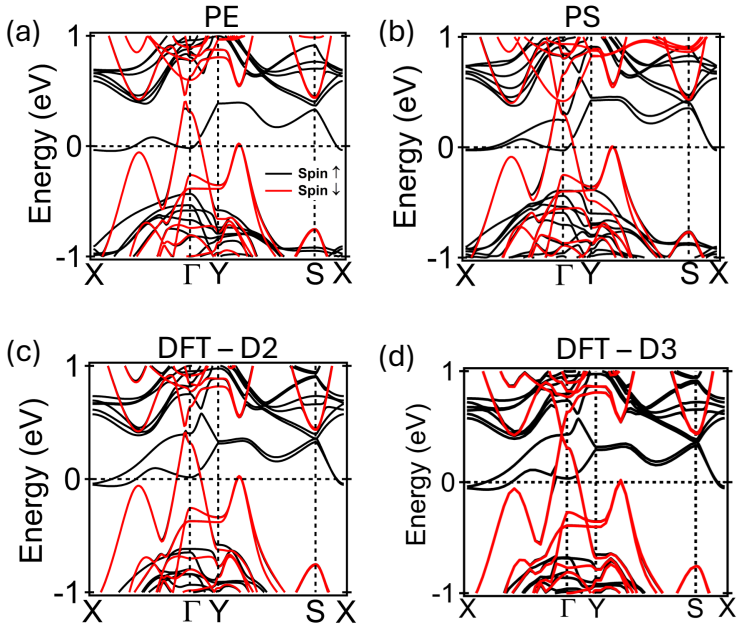

Fig. S2 Spin - polarized band structures of the $ZrTe_5$/CrSBr heterostructure calculated using different exchange - correlation functionals and dispersion correction methods: (a) PBE, (b) PBEsol, (c) DFT - D2, and (d) DFT - D3 with Hubbard U = 4 eV and J = 1 eV.

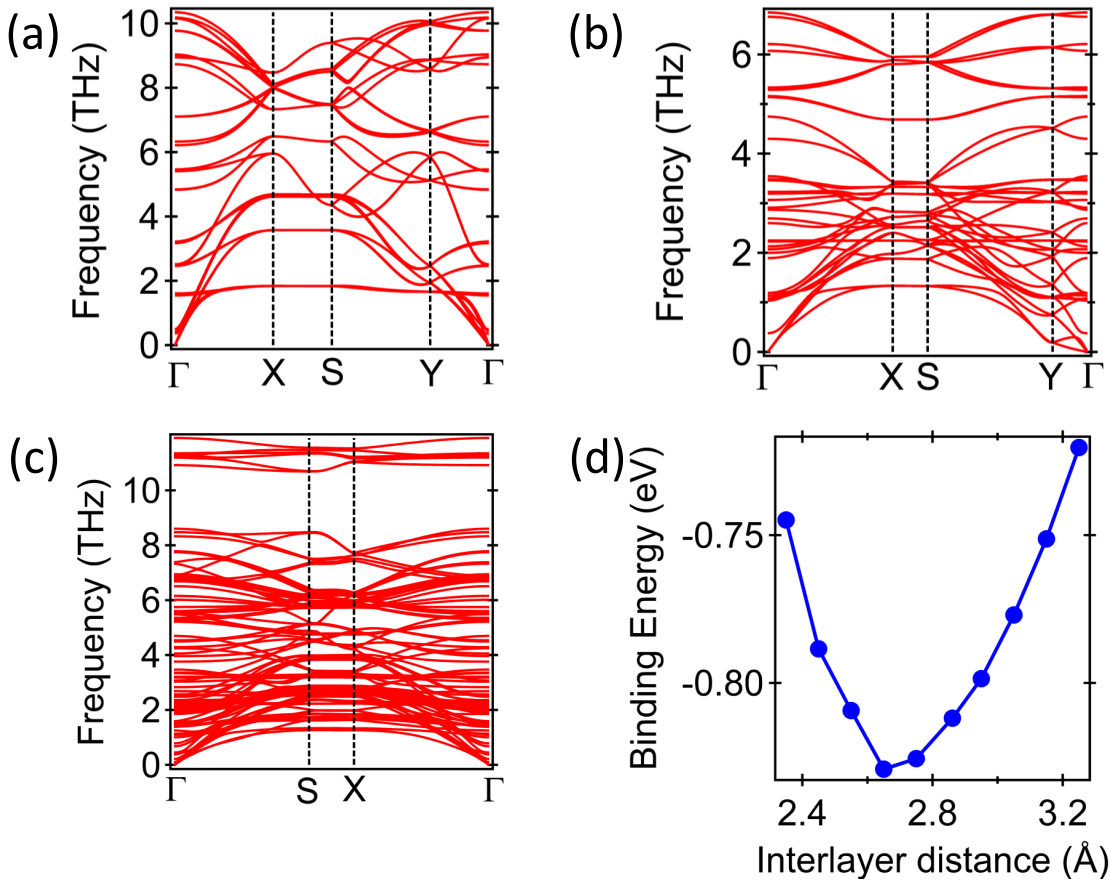

Fig. S3 Phonon band structure for (a) monolayer CrSBr, (b) monolayer $ZrTe_5$, and (c) the $ZrTe_5$/CrSBr heterostucture. (d) Binding energy as a function of interlayer distance for the $ZrTe_5$/CrSBr heterostucture.

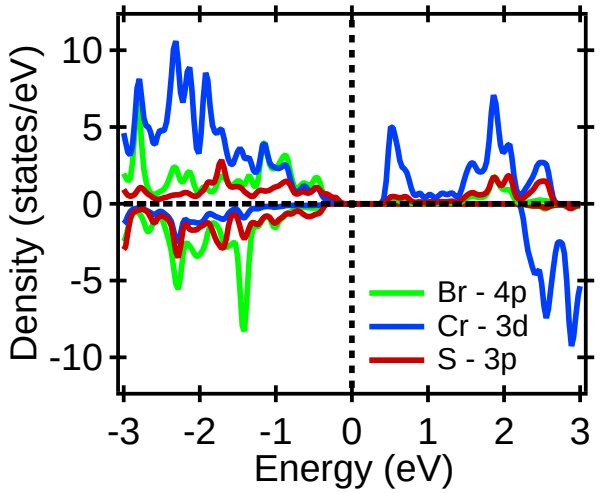

Fig. S4 Projected Density of States (PDOS) of the monolayer CrSBr.

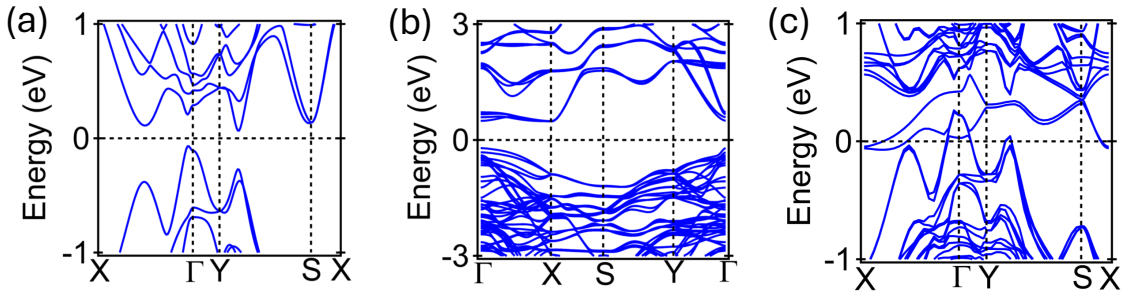

Fig. S5 Spin – orbit coupling (SOC) band structures of: (a) monolayer $ZrTe_5$, (b) monolayer CrSBr, and (c)$ZrTe_5$/CrSBr heterostructure.

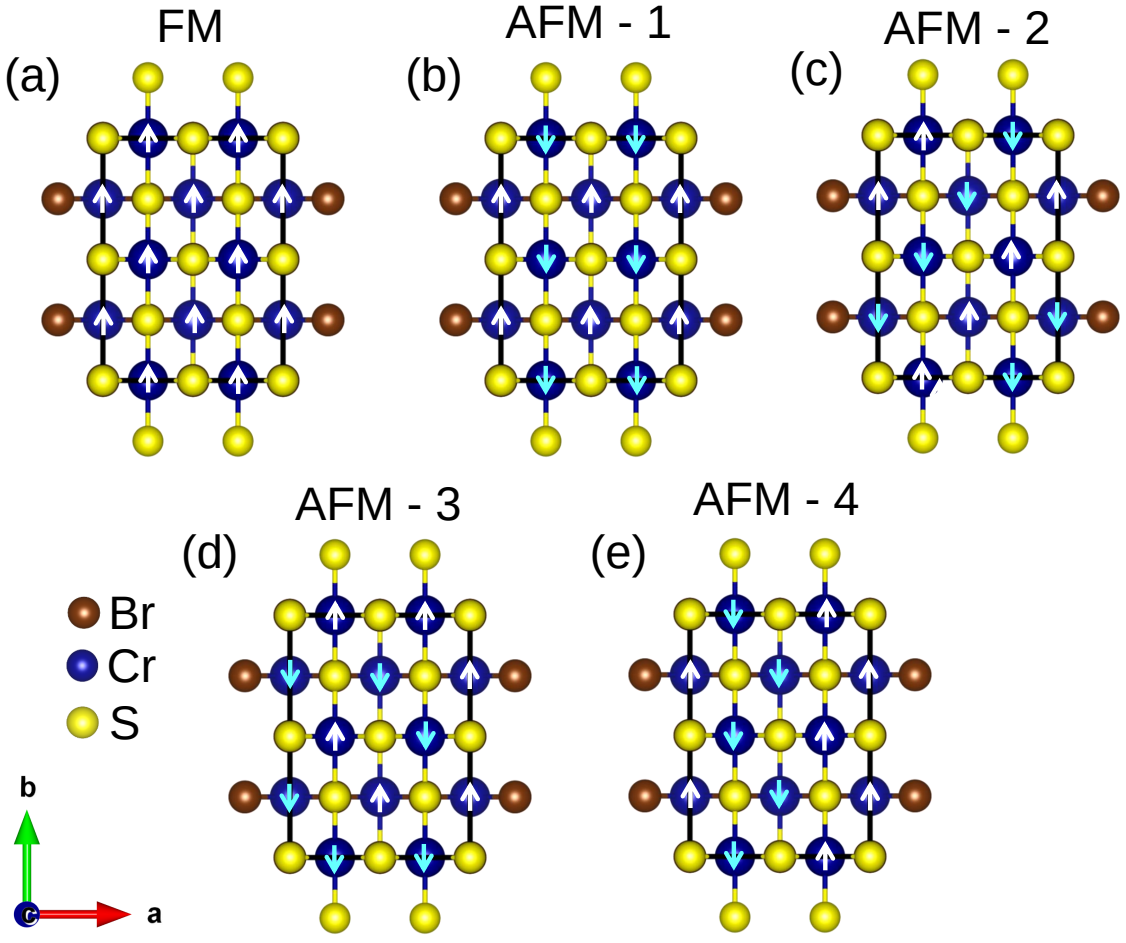

Fig. S6 Various ferromagnetic (FM) and antiferromagnetic (AFM) configurations of the 2 × 2 CrSBr supercell.

Table S1 Total energies of various FM and AFM configurations.

Configuration	CrSBr	$ZrTe_5$/CrSBr
FM	-127.042 eV	-153.914 eV
AFM - 1	-126.747 eV	-153.458 eV
AFM - 2	-126.621 eV	-153.464 eV
AFM - 3	-126.613 eV	-153.447 eV
AFM - 4	-126.544 eV	-153.460 eV

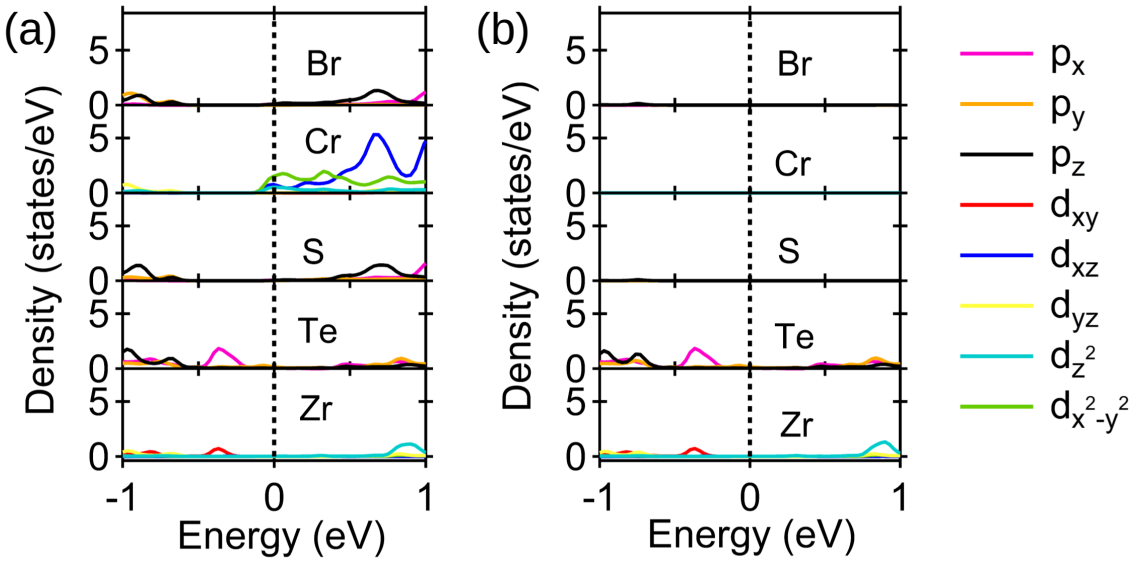

Fig. S7 Projected Density of States (PDOS) for the $ZrTe_5$/CrSBr heterostructure.

Table S2 The binding energy of the parallel (P) and antiparallel (AP) configurations in the CrSBr/nL - $ZrTe_5$/CrSBr heterostucture

Configuration	P (eV)	AP (eV)
CrSBr/1L-$ZrTe_5$/CrSBr	-3.10178	-2.17972
CrSBr/2L-$ZrTe_5$/CrSBr	-5.44192	-4.51792
CrSBr/3L-$ZrTe_5$/CrSBr	-7.82737	-6.89963
CrSBr/4L-$ZrTe_5$/CrSBr	-10.0645	-9.18046
CrSBr/5L-$ZrTe_5$/CrSBr	-12.587	-11.5716

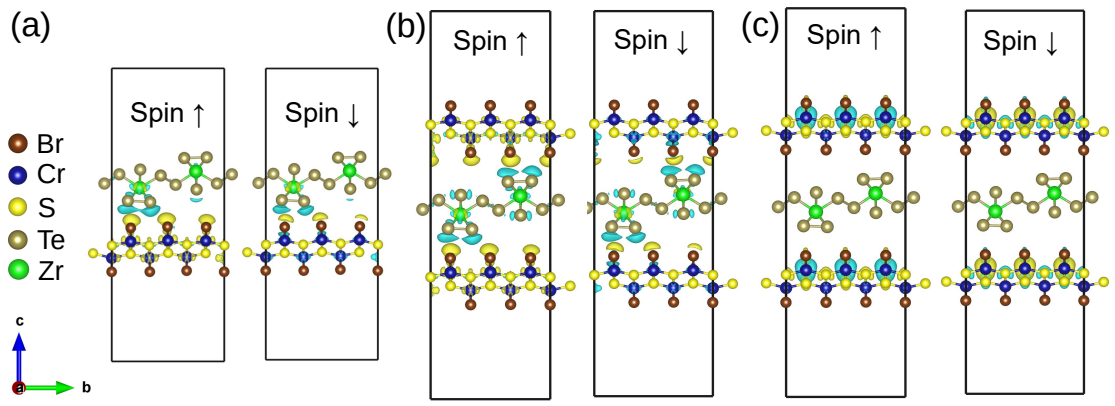

Fig. S8 Spin - dependent charge density difference for (a) $ZrTe_5$/CrSBr and the CrSBr/1L - $ZrTe_5$/CrSBr heterostucture in (b) P configuration and (c) AP configuration.

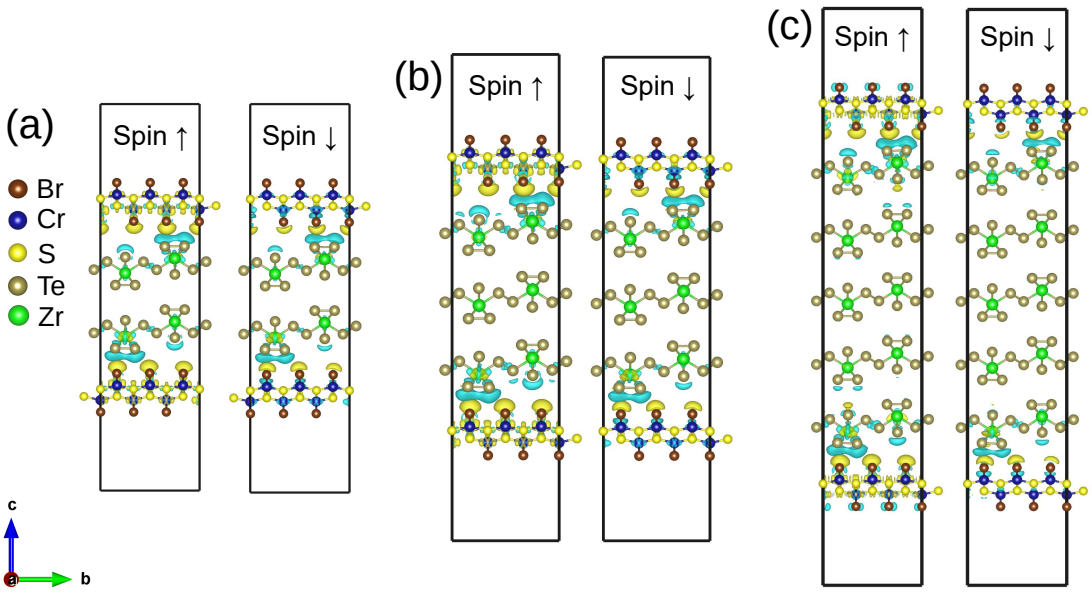

Fig. S9 Spin - dependent charge density difference for the P configuration of the heterostuctures: (a) CrSBr/2L - $ZrTe_5$/CrSBr, (b) CrSBr/3L - $ZrTe_5$/CrSBr, and (c) CrSBr/5L - $ZrTe_5$/CrSBr.

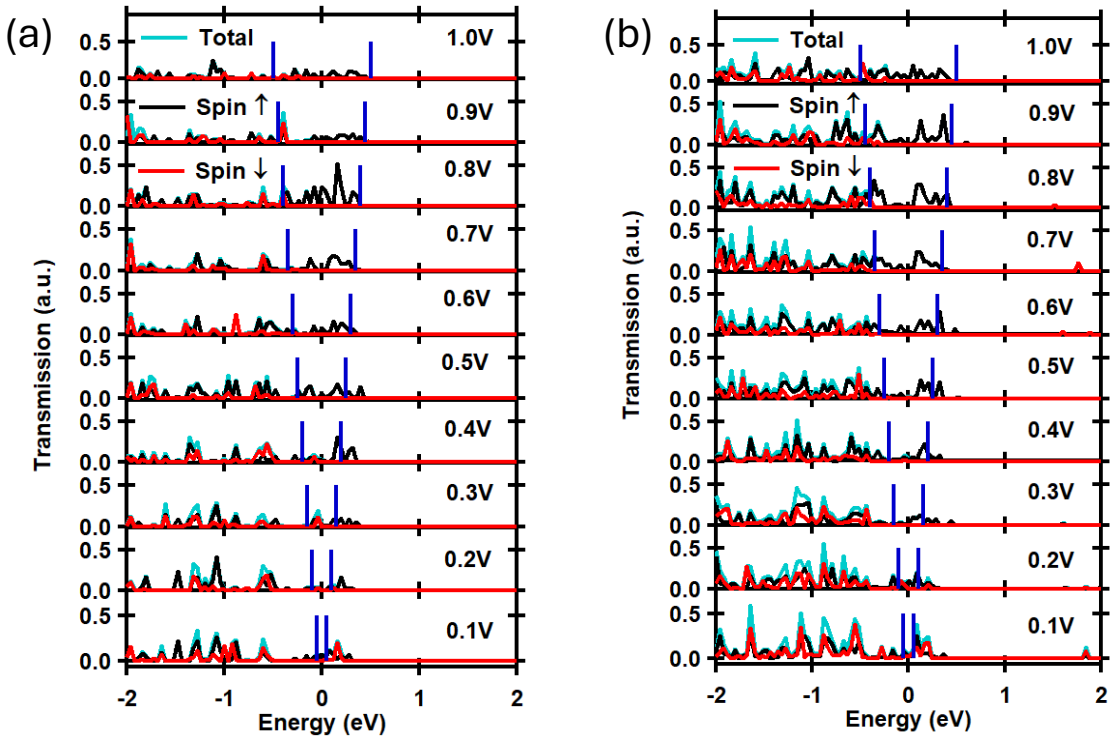

Fig. S10 Transmission spectrum in AP configuration under different bias voltages for: (a) CrSBr/5L - $ZrTe_5$/CrSBr and (b) CrSBr/$ZrTe_5$/CrSBr heterostructures.

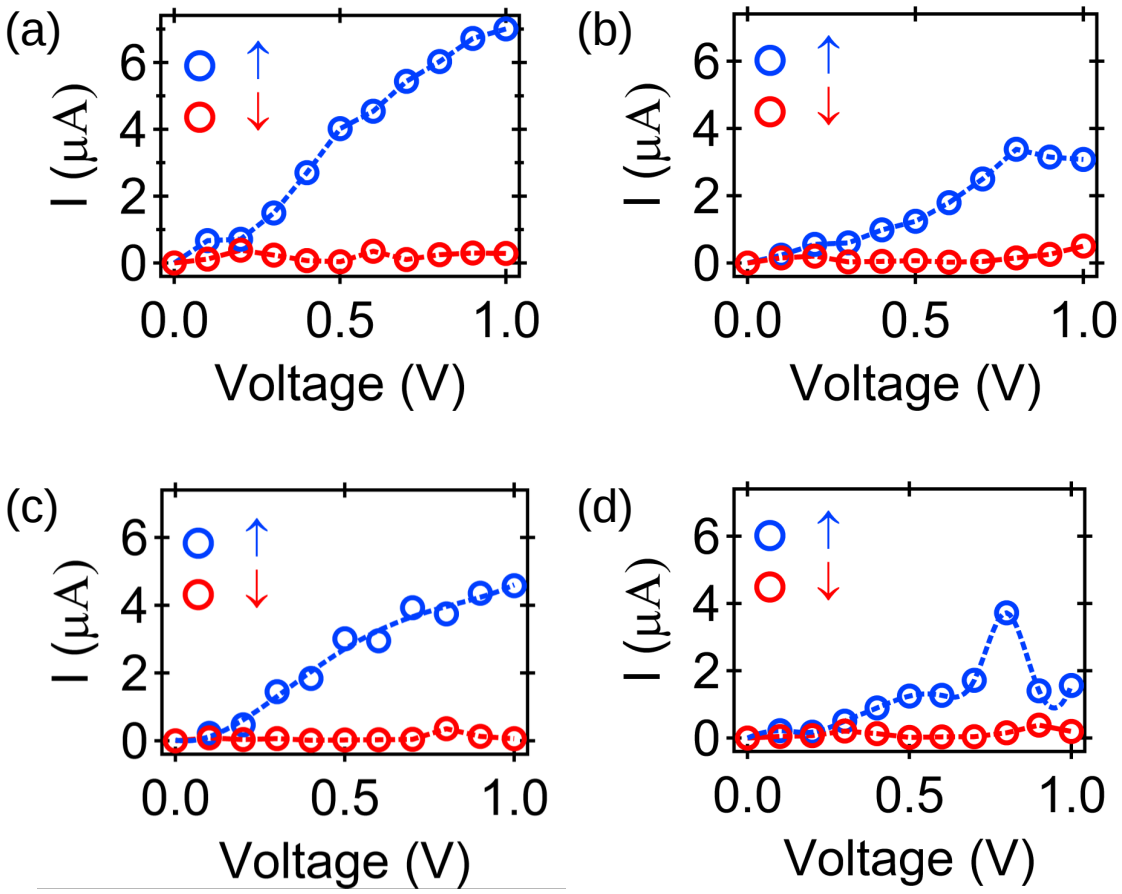

Fig. S11 IV characteristics of CrSBr/1L - $ZrTe_5$/CrSBr in (a) P and (b) AP configurations, and of CrSBr/5L - $ZrTe_5$/CrSBr in (c) P and (d) AP configurations. Scatter plots depict actual data, while dashed lines represent fitted curves.